Dust acoustic shock wave at high dust density

Samiran Ghosh, Susmita Sarkar, Manoranjan Khan, K. Avinash, and M. R. Gupta

Citation: Physics of Plasmas (1994-present) **10**, 977 (2003); doi: 10.1063/1.1555621
View online: http://dx.doi.org/10.1063/1.1555621
View Table of Contents: http://scitation.aip.org/content/aip/journal/pop/10/4?ver=pdfcov
Published by the AIP Publishing

Dust acoustic shock wave at high dust density

Samiran Ghosh,[a] Susmita Sarkar,[b] Manoranjan Khan,[c] K. Avinash,[d] and M. R. Gupta
Centre for Plasma Studies, Faculty of Science, Jadavpur University Calcutta-7000 032, India

(Received 12 August 2002; accepted 30 December 2002)

Dust acoustic (DA) shock wave at high dust density, i.e., the dust electroacoustic (DEA) or dust Coulomb (DC) shock wave has been investigated incorporating the nonadiabatic dust charge variation. The nonlinear DEA (DC) shock wave is seen to be governed by the Korteweg–de Vries Burger equation, in which the Burger term is proportional to the nonadiabaticity generated dissipation. It is seen that the shock strength decreases but after reaching minimum, it increases as the dust space charge density $|q_d n_d|$ increases and the shock strength of DA wave is greater than that of DEA (DC) wave. Moreover the DEA (DC) shock width increases appreciably with increase mass m_i of the ion component of the dusty plasma but for DA shock wave the effect is weak. © *2003 American Institute of Physics.* [DOI: 10.1063/1.1555621]

I. INTRODUCTION

In a dusty plasma, it is through the capture collisions with plasma electrons and ions that electric charge gathers on the dust grain surface and so is subjected to fluctuations. Hence the charge q_d on the dust surface is an extra dynamical variable and is determined by the dust charging equation

$$f(\phi,q_d)\equiv I_e(\phi,q_d)+I_i(\phi,q_d)=\frac{dq_d}{dt}, \tag{1}$$

where

$$I_e(\phi,q_d)=-\pi a^2 e\sqrt{\frac{8T_e}{\pi m_e}}n_e(\phi)\exp\left(\frac{eq_d}{4\pi\epsilon_0 aT_e}\right),$$
$$I_i(\phi,q_d)=\pi a^2 e\sqrt{\frac{8T_i}{\pi m_i}}n_i(\phi)\left(1-\frac{eq_d}{4\pi\epsilon_0 aT_i}\right) \tag{2}$$

are the electron, ion currents, respectively, and $4\pi\epsilon_0 a$ is the capacitance of the charged dust grain of radius a. The dust density n_d at the same potential ϕ is fixed up by the charge neutrality condition

$$g(\phi,q_d,n_d)\equiv en_i(\phi)-en_e(\phi)+q_d n_d=0 \tag{3}$$

when the density scale length of the dust cloud is large in comparison to the plasma Debye length λ_D. On the other hand, if the density scale length of the dust cloud is comparable to the plasma Debye length (λ_D), the dust density n_d at ϕ is fixed up by the Poisson equation:

$$g(\phi,q_d,n_d)\equiv en_i(\phi)-en_e(\phi)+q_d n_d=\frac{\partial^2\phi}{\partial x^2},$$
$$n_i(\phi)=n_0\exp\left(-\frac{e\phi}{T_i}\right),\quad n_e(\phi)=n_0\exp\left(\frac{e\phi}{T_e}\right). \tag{4}$$

Here $n_i(\phi)$ and $n_e(\phi)$ are the ion and electron number densities corresponding to Boltzmann distribution in electrostatic potential ϕ at temperature T_i and T_e, respectively. We have made the choice $n_i(\phi=0)=n_e(\phi=0)=n_0$[1] so that in the limit $\phi\to 0$ we get $n_d\to 0$; there is practically no dust and consequently the electron and ion number densities are the same. In this state defined by $I_e+I_i=0$ with $\phi\to 0$ so that $n_d\to 0$ the charge $q_d=-z_{d0}e$ is the equilibrium charge on a single dust grain. This situation describes a highly tenuous dusty plasma. On the other hand, to describe the equilibrium state with not too low dust density or sufficiently high dust density one may choose an appropriate negative (constant) value of ϕ_0 so that the electron and ion densities are no longer equal. The corresponding equilibrium q_{d0} on a dust grain surface is to be obtained from $I_e+I_i=0$ with electron–ion density ratio$=\exp[e\phi_0(1/T_e+1/T_i)]$. Clearly $|q_{d0}|<z_{d0}e$. In general $(T_e/e)[\sigma/(\sigma+1)]\ln(\sqrt{\sigma m_e/m_i})<\phi_0<0$ and $-z_{d0}e<q_{d0}<0$, while the end values correspond to very low or sufficiently high dust densities as the case may be.

At the relatively high dust density region, the magnitude of the charge (negative) on the surface of a dust grain is much lower than the charge on a isolated dust grain surface,[2–4] i.e., $d(q_d)/dn_d<0$. At high dust density the dust charge q_d and electrostatic potential ϕ exhibits strong functional dependence of n_d as shown by Goertz[1] and Havnes *et al.*,[5] but the dependence is very weak at relatively low dust density.[6–10] This functional dependence of $\phi(n_d)$ and $q_d(n_d)$ on n_d can support a very low frequency wave mode called dust electroacoustic (DEA) wave[11,12] in a dusty plasma which has no existence in a three component plasma with fixed charge on the dust grains. The problem of dust acoustic (DA) wave propagation at high dust density named dust Coulomb (DC) wave was also considered earlier.[13–15] It has been shown[16] that DEA and DC waves are equivalent at least in the linear approximation and have the same dispersion relation. A Boussinesq equation was derived describing the nonlinear behavior of the DCW[17] but this was done ignoring the contribution of order ω_{pd}/ν_{ch} in the dust charging equa-

[a]Electronic mail: sran@jufs.ernet.in and sran_g@yahoo.com
[b]Department of Applied Mathematics, University of Calcutta, 92, A.P.C. Road, Calcutta-7000 009 India.
[c]Electronic mail: mk@jufs.ernet.in and mkhan_ju@yahoo.com
[d]Institute for Plasma Research, Gandhinagar 382428, India.

tion and consequently neglecting the anomalous dissipation effect resulting from dust charge variations ($\sim \partial q_d/\partial t$) which gives rise to the Burger term and makes possible shock wave generation in a dusty plasma.

Equations (1) and (3) or (4) indicate that the potential $\phi(n_d)$ and dust grain charge $q_d(n_d)$ are functions of the dust density n_d. In the linear analysis of DEA wave, it was assumed[11,12] that the dust density scale length is large in comparison to the plasma Debye length (λ_D) so that Poission equation (4) was approximated $g(\phi,q_d,n_d)=0$ [charge neutrality condition (3)] and hence the linear DEA wave presented there became dispersionless. However, to study the nonlinear wave process in a plasma, it is necessary to consider the dispersive effect of the wave for balancing the nonlinear induced wave breaking effect. Recently this has been done[18] replacing the charge neutrality equation (3) by Poisson's equation (4) and thereby incorporating the dispersive effect saturating the dust fluid convection induced nonlinear wave front steepening effect, while the dust charge variation is taken to be adiabatic,[19,20] which implies replacement of Eq. (1) by

$$I_e+I_i=\frac{dq_d}{dt}=O\left(\frac{\omega_{\rm pd}}{\nu_{\rm ch}}\right)=0$$

a reasonably valid approximation where $\omega_{\rm pd}/\nu_{\rm ch}\ll 1$.

In this paper the effect of nonadiabatic dust charge variation on nonlinear DA waves at high dust density, i.e., DEA (DC) waves, has been studied under the assumption that the ratio of dust plasma frequency ($\omega_{\rm pd}$) to the dust charging frequency ($\nu_{\rm ch}$) is small but finite [$\omega_{\rm pd}/\nu_{\rm ch}\approx O(\sqrt{\epsilon})$, ϵ being the usual expansion parameter]. Thus we are to consider both the full dust charging equation (1) and Poisson's equation (4) to determine the nonlinear contributions in case of high dust density when ϕ as well as q_d are to be treated as functional of n_d. The nonadiabatic dust charge variation plays a dissipative role in a truly dusty plasma and thus leads to the formation of shock wave[21–23] in a dusty plasma. The nonlinear DEA (DC) shock wave is seen to be governed by the Korteweg–deVries (KdV) Burger equation and the generated DEA (DC) shock wave is compressional which provides sufficient dust density enhancement in a dusty plasma.

II. THE MODEL

To formulate the physical problem we introduce the following normalized space time and other dynamical variables:

$$T=\omega_{\rm pd}t,\quad X=\frac{x}{\lambda_c},\quad V_d=\frac{v_d}{c_{\rm dea}},\quad N_d=\frac{n_d}{n_{d0}},$$
$$\Phi=\frac{e\phi}{T_e},\quad Q=\frac{q_d}{z_{d0}e},\quad \sigma=\frac{T_i}{T_e},\quad z_0=\frac{z_{d0}e^2}{4\pi\epsilon_0 aT_e},\tag{5}$$
$$T_{\rm eff}=T_e\left(z_{d0}QN_d\frac{d\Phi}{dN_d}\right)_0.$$

Here $q_d=z_{d0}eQ$. At low dust density, i.e., when $n_d\to 0$ with $\phi\to 0$, $Q\to -1$ so that the equilibrium charge on a single dust grain is $-z_{d0}e$, $\omega_{\rm pd}=\sqrt{n_{d0}z_{d0}^2e^2/\epsilon_0 m_d}$ is the dust plasma frequency, $c_{\rm dea}$ is the linear DEA wave velocity, $T_{\rm eff}$ is the effective temperature associated with the dust pressure gradient—the latter role being played by the electrostatic potential gradient force due to the functional dependence of Φ on N_d and $\lambda_c=\sqrt{\epsilon_0 T_{\rm eff}/n_{d0}z_{d0}^2e^2}$ is the dust space charge self-shielding length.

In terms of the normalized variables the dust fluid equations are

$$\frac{\partial N_d}{\partial T}+\frac{\partial(N_dV_d)}{\partial X}=0,\tag{6}$$

$$\frac{\partial V_d}{\partial T}+V_d\frac{\partial V_d}{\partial X}=-\frac{T_ez_{d0}Q}{T_{\rm eff}}\frac{\partial\Phi}{\partial X}.\tag{7}$$

The dust charging equation (1) and the Poisson's equation (4) becomes

$$f(\Phi,Q)\equiv\exp\left[\left(1+\frac{1}{\sigma}\right)\Phi\right]-\sqrt{\sigma}\sqrt{\frac{m_e}{m_i}}\left(1-\frac{z_0}{\sigma}Q\right)e^{-z_0Q}$$
$$=-\frac{z_0(1+z_0+\sigma)}{\sqrt{\sigma}}\sqrt{\frac{m_e}{m_i}}\exp\left(\frac{\Phi}{\sigma}-z_0Q\right)\left(\frac{\omega_{\rm pd}}{\nu_{\rm ch}}\right)\frac{dQ}{dT},\tag{8}$$

$$g(\Phi,Q,N_d)\equiv\exp(\Phi)-\exp\left(-\frac{\Phi}{\sigma}\right)-\delta QN_d=\frac{\lambda_D^2}{\lambda_c^2}\frac{\partial^2\Phi}{\partial X^2},\tag{9}$$

where

$$\delta=\frac{z_{d0}n_{d0}}{n_0},\quad \lambda_D=\sqrt{\frac{\epsilon_0T_e\sigma}{n_0e^2(\sigma+1)}},$$
$$\nu_{\rm ch}=\frac{a}{2\pi}\frac{\omega_{\rm pi}}{\lambda_{\rm Di}}(1+\sigma-z_0Q_0)\tag{10}$$

where λ_D is the plasma Debye shielding length, $\nu_{\rm ch}$ is the dust charging frequency, $\omega_{\rm pi}$ is the ion plasma frequency, and $\lambda_{\rm Di}$ is the ion Debye length.

We consider small but finite amplitude perturbations ΔN_d, ΔV_d, $\Delta\Phi$, and ΔQ about the unperturbed steady state defined by

$$N_{d0}=1,\quad V_d=0,\quad \Phi_0=\Phi(N_{d0}),\quad Q_0=Q(N_{d0}).\tag{11}$$

We employ the usual reductive perturbation technique and introduce the perturbation expansions

$$\Delta H=\epsilon\Delta H^{(1)}+\epsilon^2\Delta H^{(2)}+\cdots,\tag{12}$$

where $H=N_d,V_d,Q$ and the stretched variables are[21–23]

$$\xi=\sqrt{\epsilon}(X-\lambda T),\quad \tau=\epsilon^{3/2}T,\quad \frac{\omega_{\rm pd}}{\nu_{\rm ch}}=\nu\sqrt{\epsilon},\tag{13}$$

where $\nu\approx O(1)$.

We now need to express $\Delta\Phi$ and ΔQ in terms of ΔN_d to $O(\epsilon^2)$ and also retain the dispersive effect from

$$f(\Phi_0+\Delta\Phi,Q_0+\Delta Q)=-\Delta_{\rm ch},\tag{14}$$

$$g(\Phi_0+\Delta\Phi,Q_0+\Delta Q,N_{d0}+\Delta N_d)=\Delta',\tag{15}$$

where

$$\Delta_{\rm ch}=\nu\sqrt{\epsilon}A\exp\left(\frac{\Delta\Phi}{\sigma}-z_0\Delta Q\right)\times\left[\epsilon^{3/2}\frac{\partial}{\partial\tau}+\sqrt{\epsilon}(\Delta V_d-\lambda)\frac{\partial}{\partial\xi}\right]\Delta Q, \tag{16}$$

$$\Delta'=\epsilon\frac{\lambda_D^2}{\lambda_c^2}\frac{\partial^2\Delta\Phi}{\partial\xi^2}$$

and

$$A=\frac{z_0(1+z_0+\sigma)}{(z_0+\sigma)}e^{\Phi_0}. \tag{17}$$

Taylor expansion of (14) and (15) yields

$$f_{\Phi_0}\Delta\Phi+f_{Q_0}\Delta Q+F+\Delta_{\rm ch}=0, \tag{18}$$

$$g_{\Phi_0}\Delta\Phi+g_{Q_0}\Delta Q+g_{N_{d0}}\Delta N_d+C-\Delta'=0, \tag{19}$$

where

$$F=\tfrac{1}{2}[f_{\Phi_0\Phi_0}(\Delta\Phi)^2+f_{Q_0Q_0}(\Delta Q)^2], \tag{20}$$

$$C=\tfrac{1}{2}[g_{\Phi_0\Phi_0}(\Delta\Phi)^2+2g_{Q_0Nd0}\Delta Q\Delta N_d]. \tag{21}$$

In obtaining (20) and (21) it is to be noted that $f_{Q\Phi}$, g_{QQ}, $g_{Q\Phi}$, $g_{N_dN_d}$, and $g_{\Phi N_d}$ vanish identically. By solving $\Delta\Phi$ and ΔQ are next expressed in the following form:

$$\Delta\Phi=\frac{f_{Q_0}}{J}[g_{N_{d0}}\Delta N_d+C-\Delta']-\frac{g_{Q_0}}{J}[F+\Delta_{\rm ch}], \tag{22}$$

$$\Delta Q=\frac{f_{\Phi_0}}{J}[g_{N_{d0}}\Delta N_d+C-\Delta']+\frac{g_{\Phi_0}}{J}[F+\Delta_{\rm ch}], \tag{23}$$

where J is the Jacobian given by

$$J=\left.\frac{\partial(f,g)}{\partial(\Phi,Q)}\right|_0 \tag{24}$$

while the partial derivatives are

$$\begin{aligned}
f_\Phi&=\left(1+\frac{1}{\sigma}\right)\exp\left[\left(1+\frac{1}{\sigma}\right)\Phi\right],\\
f_{\Phi\Phi}&=\left(1+\frac{1}{\sigma}\right)^2\exp\left[\left(1+\frac{2}{\sigma}\right)\Phi\right],\\
f_Q&=\frac{z_0(1+\sigma-z_0Q)}{\sigma-z_0Q}\exp\left[\left(1+\frac{1}{\sigma}\right)\Phi\right],\\
f_{QQ}&=\frac{z_0^2(2+\sigma-z_0Q)}{\sigma-z_0Q}\exp\left[\left(1+\frac{1}{\sigma}\right)\Phi\right],\\
g_{\Phi_0}&=\exp(\Phi_0)+\frac{1}{\sigma}\exp\left(-\frac{\Phi_0}{\sigma}\right),\\
g_{Q_0}&=-\delta N_{d0},\\
g_{N_{d0}}&=-\delta Q_0,\\
g_{\Phi_0\Phi_0}&=\exp(\Phi_0)-\frac{1}{\sigma^2}\exp\left(-\frac{\Phi_0}{\sigma}\right).
\end{aligned} \tag{25}$$

On using the perturbation given by (12), we get the following expansions for $\Delta\Phi$ and ΔQ:

$$\begin{aligned}
\Delta\Phi&=\epsilon\Delta\Phi^{(1)}+\epsilon^2\Delta\Phi^{(2)},\\
\Delta Q&=\epsilon\Delta Q^{(1)}+\epsilon^2\Delta Q^{(2)}
\end{aligned} \tag{26}$$

with

$$\Delta\Phi^{(1)}=\frac{d\Phi}{dN_d}\Delta N_d^{(1)},\quad \Delta Q^{(1)}=\frac{dQ}{dN_d}\Delta N_d^{(1)}, \tag{27}$$

$$\begin{aligned}
\Delta\Phi^{(2)}=&\frac{d\Phi}{dN_d}\Delta N_d^{(2)}+\frac{1}{2}\frac{d^2\Phi}{dN_d^2}(\Delta N_d^{(1)})^2\\
&-\frac{\lambda_D^2}{\lambda_c^2}\frac{f_Q}{J}\frac{d\Phi}{dN_d}\frac{\partial^2\Delta N_d^{(1)}}{\partial\xi^2}\\
&+\nu\lambda A\frac{g_Q}{J}\frac{dQ}{dN_d}\frac{\partial\Delta N_d^{(1)}}{\partial\xi},
\end{aligned} \tag{28}$$

$$\begin{aligned}
\Delta Q^{(2)}=&\frac{dQ}{dN_d}\Delta N_d^{(2)}+\frac{1}{2}\frac{d^2Q}{dN_d^2}(\Delta N_d^{(1)})^2\\
&+\frac{\lambda_D^2}{\lambda_c^2}\frac{f_\Phi}{J}\frac{dQ}{dN_d}\frac{\partial^2\Delta N_d^{(1)}}{\partial\xi^2}\\
&-\nu\lambda A\frac{g_\Phi}{J}\frac{dQ}{dN_d}\frac{\partial\Delta N_d^{(1)}}{\partial\xi}.
\end{aligned} \tag{29}$$

The explicit expressions for $(d\Phi/dN_d)_0$, $(dQ/dN_d)_0$, J are now obtained from (22) and (23) by applying the usual rules of partial derivatives and using the partial derivatives given by (25),

$$J=-e^{[1+(1/\sigma)]\Phi_0}\left[\delta\left(1+\frac{1}{\sigma}\right)+\frac{z_0(1+\sigma-z_0Q_0)}{\sigma-z_0Q_0}\times\left(e^{\Phi_0}+\frac{1}{\sigma}e^{-(\Phi_0/\sigma)}\right)\right], \tag{30}$$

$$\left(\frac{d\Phi}{dN_d}\right)_0=g_{N_{d0}}\frac{f_{Q_0}}{J}=-\frac{1}{J}\frac{\delta Q_0z_0(1+\sigma-z_0Q_0)}{\sigma-z_0Q_0}, \tag{31}$$

$$\left(\frac{dQ}{dN_d}\right)_0=-g_{N_{d0}}\frac{f_{\Phi_0}}{J}=\frac{\delta Q_0}{J}e^{-(1+1/\sigma)\Phi_0}. \tag{32}$$

To compare with earlier results,[13,16] we calculate the phase velocity λ of the linear nondispersive wave

$$\lambda^2=\frac{T_{\rm eff}}{m_d}=\frac{T_e}{m_d}\left(z_{d0}QN_d\frac{d\Phi}{dN_d}\right)_0=\frac{T_e}{m_d}\frac{\delta z_{d0}Q_0^2}{\dfrac{\delta(1+\sigma)(\sigma-z_0Q_0)}{z_0\sigma(1+\sigma-z_0Q_0)}+\left(e^{\Phi_0}+\dfrac{1}{\sigma}e^{-\Phi_0/\sigma}\right)}. \tag{33}$$

Setting $\delta=z_{d0}n_{d0}/n_0$ [Eq. (10)] and $z_0=z_{d0}e^2/4\pi\epsilon_0aT_e$ [Eq. (5)] and changing from our notations to those of Refs.

13 and 16 by the replacement $n_0 \exp(\Phi_0) \rightarrow n_{e0}$, $n_0 \exp(-\Phi_0/\sigma) \rightarrow n_{i0}$, and $Q_0 \rightarrow -1$, the ratio of ω_2 and ω_1 as defined in Refs. 13 and 16 is found to be

$$\frac{\omega_2}{\omega_1} = \frac{(\sigma + z_0)(1+\sigma)}{\sigma(1+z_0+\sigma)}. \tag{34}$$

So the RHS of (33) equals

$$\lambda^2 = \frac{\omega_{\mathrm{pd}}^2}{[\lambda_{\mathrm{De}}^{-2} + \lambda_{\mathrm{Di}}^{-2} + (\omega_2/\omega_1)\ (f/\lambda_D^2)]} = \frac{\omega_{\mathrm{pd}}^2}{\lambda_D^{-2} + \lambda_c^{-2}}, \tag{35}$$

where $f = n_{d0} a \lambda_D^2$ is the so-called fugacity parameter.[13] This also correctly introduces the new length scale λ_c associated with DCW[17]

$$\frac{1}{\lambda_c^2} = \frac{\omega_2}{\omega_1}\frac{f}{\lambda_D^2} = n_{d0} a \left(\frac{\omega_2}{\omega_1}\right). \tag{36}$$

Thus although our presentations are seemingly suitable for high dust density, they are equally applicable for all dust densities, high, low or belonging to the intermediate range.

The higher order derivatives are obtainable from the following formulas (insert suffix zero for equilibrium value):

$$\frac{d^2\Phi}{dN_d^2} = \frac{1}{J}\left[f_Q \left(g_{\Phi\Phi}\left(\frac{d\Phi}{dN_d}\right)^2 + 2 g_{QN_d}\frac{dQ}{dN_d}\right) - g_Q\left(f_{\Phi\Phi}\left(\frac{d\Phi}{dN_d}\right)^2 + f_{QQ}\left(\frac{dQ}{dN_d}\right)^2\right)\right], \tag{37}$$

$$\frac{d^2Q}{dN_d^2} = \frac{1}{J}\left[g_\Phi \left(f_{\Phi\Phi}\left(\frac{d\Phi}{dN_d}\right)^2 + f_{QQ}\left(\frac{dQ}{dN_d}\right)^2\right) - f_\Phi\left(g_{\Phi\Phi}\left(\frac{d\Phi}{dN_d}\right)^2 + 2 g_{QN_d}\frac{dQ}{dN_d}\right)\right], \tag{38}$$

by substituting for $d\Phi/dN_d$, dQ/dN_d and the partial and mixed derivatives, using (25), (31), and (32). We refrain from giving the algebraic form as it is much convenient to calculate the values numerically as in any case the resulting equation (KdV Burger) is not exactly solvable and we have to fall on numerical computation.

Substituting in the dust fluid equations (6) and (7) the expressions for ΔN_d, ΔV_d, $\Delta\Phi$, and ΔQ given in (12), (26)–(29), expressing $\partial/\partial X$, $\partial/\partial T$ in terms of derivatives with respect to stretched variables and using local approximation, we obtain the following equations:

$$O(\epsilon^{3/2}): \quad \Delta V_d^{(1)} = \Delta N_d^{(1)}, \quad \lambda = 1. \tag{39}$$

Equations of the $O(\epsilon^{5/2})$ are

$$\frac{\partial \Delta N_d^{(1)}}{\partial \tau} + \frac{\partial(\Delta N_d^{(1)} \Delta V_d^{(1)})}{\partial \xi} = \frac{\partial(\Delta N_d^{(2)} - \Delta V_d^{(2)})}{\partial \xi} \tag{40}$$

and

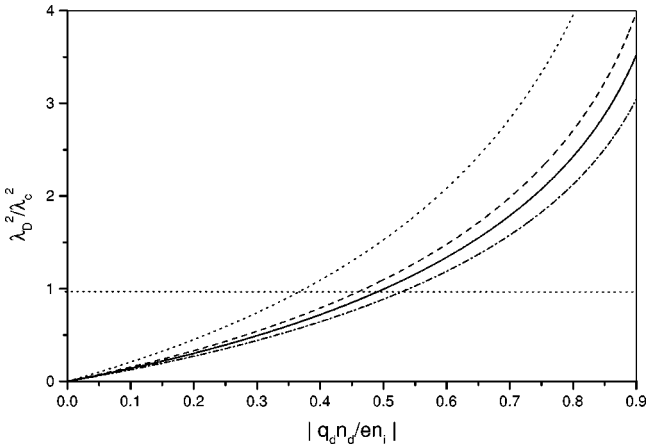

FIG. 1. Variation of λ_D^2/λ_c^2 as a function of $|q_d n_d/en_i|$ for $\sigma = T_i/T_e = 0.1$. Dotted line, dashed line, solid line, and dashed–dotted lines represent the curves for hydrogen, oxygen, argon, and cesium plasma, respectively. The horizontal dotted line represents the line $\lambda_D^2/\lambda_c^2 = 1$.

$$\frac{\partial \Delta V_d^{(1)}}{\partial \tau} + \Delta V_d^{(1)}\frac{\partial \Delta V_d^{(1)}}{\partial \xi} = \frac{\partial(\Delta V_d^{(2)} - \Delta N_d^{(2)})}{\partial \xi} - \frac{d}{dN_d}\left[\ln\left(Q\frac{d\Phi}{dN_d}\right)\right]\Delta N_d^{(1)}\frac{\partial \Delta N_d^{(1)}}{\partial \xi} + \frac{\lambda_D^2}{\lambda_c^2}\frac{f_Q}{J}\frac{\partial^3 \Delta N_d^{(1)}}{\partial \xi^3} - \nu A\left(\frac{f_\Phi}{f_Q}\right)\frac{g_Q}{J}\frac{\partial^2 \Delta N_d^{(1)}}{\partial \xi^2}. \tag{41}$$

Eliminating $\Delta N_d^{(2)} - \Delta V_d^{(2)}$ from (40) and (41), we finally obtain the Korteweg–de Vries Burger equation describing the DEA (DC) shock wave propagation

$$\frac{\partial \Delta N_d^{(1)}}{\partial \tau} + \alpha \Delta N_d^{(1)}\frac{\partial \Delta N_d^{(1)}}{\partial \xi} + \beta\frac{\partial^3 \Delta N_d^{(1)}}{\partial \xi^3} = \mu\frac{\partial^2 \Delta N_d^{(1)}}{\partial \xi^2}, \tag{42}$$

where

$$\alpha = \frac{3}{2} + \frac{1}{2}\frac{d}{dN_d}\ln\left(Q\frac{d\Phi}{dN_d}\right),$$

$$\beta = -\frac{1}{2}\frac{\lambda_D^2}{\lambda_c^2}\frac{f_Q}{J}, \tag{43}$$

$$\mu = \frac{\nu}{2}\left(\frac{f_\Phi}{f_Q}\right)\frac{g_Q}{J}\frac{z_0(1+z_0+\sigma)}{(z_0+\sigma)}e^{\Phi_0}.$$

Equation (42) describes the propagation of DA shock wave when dust density is low and DEA (DC) shock waves for high dust density. The transition from DA wave to DEA (DC) wave occurs as the parameter

$$\left|\frac{q_d n_d}{en_i}\right| = 1 - \exp\left[\left(1 + \frac{1}{\sigma}\right)\Phi\right] \tag{44}$$

increases and the crossover from DA wave (Debye shielding dominates over dust self-shielding, i.e., $\lambda_D^2 < \lambda_c^2$) to DEA (DC) wave [dust self-shielding dominates over Debye shielding, i.e., $\lambda_D^2 > \lambda_c^2$] at the point $\lambda_D^2/\lambda_c^2 = 1$, as shown in Figs. 1 and 2 for hydrogen, oxygen, argon, and cesium plasma.

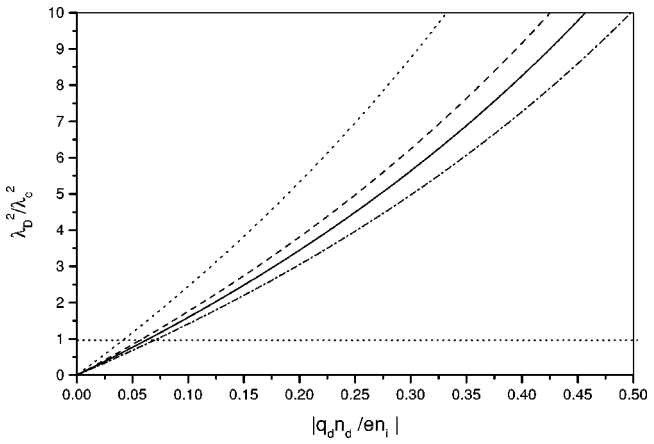

FIG. 2. Variation of λ_D^2/λ_c^2 as a function of $|q_d n_d/en_i|$ for $\sigma=0.01$. The curves are the same as in Fig. 1.

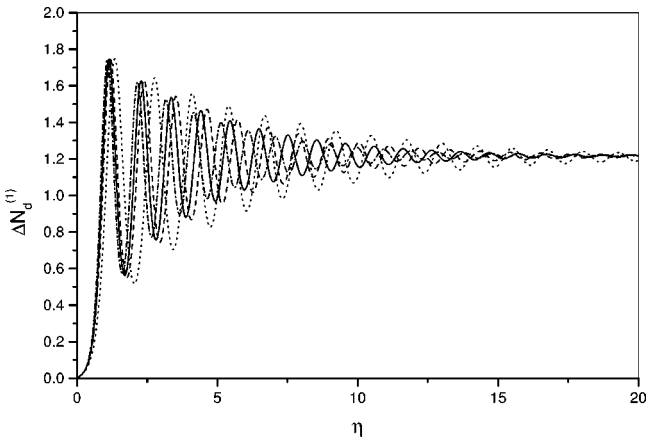

FIG. 3. Oscillatory shock structure for weak dissipation for $\sigma=0.01$ with $|q_d n_d/en_i|=0.5(\lambda_D^2/\lambda_c^2>1)$. $\Delta N_d^{(1)}$ is the normalized (normalized by equilibrium dust number density n_{d0}) dust number density and $\eta=\xi-V\tau$ is the transformed spatial cordinate. The different curves are the same as Fig. 1.

III. STEADY STATE SOLUTION

On transforming to the wave frame

$$\eta=V\tau-\xi=\sqrt{\epsilon}\frac{c_{\rm dea}(\lambda+\epsilon V)t-x}{\lambda_c} \tag{45}$$

and using the transformation $\Delta N_d^{(1)}=u$, $d\Delta N_d^{(1)}/d\eta=v$ the KdV Burger equation (42) reduces to the following set of simultaneous equations:

$$\frac{du}{d\eta}=v, \quad \frac{dv}{d\eta}=\frac{V}{\beta}u-\frac{\alpha}{2\beta}u^2-\frac{\mu}{\beta}v. \tag{46}$$

This system of equations have two singular points at $(u,v)=(0,0)$ and $(2V/\alpha,0)$. Among these two points the point (0,0) is a saddle point and $(2V/\alpha,0)$ is a stable node or a stable focus according to

$$\mu^2 > \text{or} < 4\beta V. \tag{47}$$

A stable focus implies the oscillatory shock structure, whereas stable node corresponds to a monotonic shock structure. Hence, Eqs. (13), (44), and (47) yield the following criteria for oscillatory or monotonic shock structure:

$$\frac{\lambda_D}{\lambda_c}<\left[\frac{\lambda_D}{\lambda_c}\right]_{\rm cr} \quad \text{or} \quad \frac{\lambda_D}{\lambda_c}>\left[\frac{\lambda_D}{\lambda_c}\right]_{\rm cr}. \tag{48}$$

The expression of $[\lambda_D/\lambda_c]_{\rm cr}$ is given by

$$\left[\frac{\lambda_D}{\lambda_c}\right]_{\rm cr}=\frac{\omega_{\rm pd}}{\nu_{\rm ch}}\frac{(1+z_0+\sigma)}{(z_0+\sigma)} \times\frac{e^{\Phi_0}}{\sqrt{8(M-1)}|(f_Q/J)|[(Jf_Q/f_\Phi g_Q)]^2}, \tag{49}$$

where M is the Mach number defined by

$$M=\frac{c_{\rm dea}(\lambda+\epsilon V)}{c_{\rm dea}\lambda}=1+\epsilon\frac{V}{\lambda}. \tag{50}$$

We can recognize different conditions of oscillatory or monotonic shock structure for both DA and DEA (DC) waves from Eq. (48) and from the condition of DA–DEA (DC) wave transition $\lambda_D^2/\lambda_c^2=1$. The condition for the existence of oscillatory shock of DA waves is $\lambda_D/\lambda_c<[\lambda_D/\lambda_c]_{\rm cr}\leqslant 1$, whereas the DA waves exihibits monotonic shock for $1>\lambda_D/\lambda_c>[\lambda_D/\lambda_c]_{\rm cr}$. On the other hand, the DEA (DC) waves exihibits oscillatory shock for $1<\lambda_D/\lambda_c<[\lambda_D/\lambda_c]_{\rm cr}$ and monotonic shock for $\lambda_D/\lambda_c>[\lambda_D/\lambda_c]_{\rm cr}>1$.

IV. NUMERICAL RESULTS AND DISCUSSIONS

For dusty hydrogen (dotted line), oxygen (dashed line), argon (solid line), and cesium (dashed–dotted line) plasma, Figs. 1 and 2 shows the variation of λ_D^2/λ_c^2, the ratio of Debye shielding length to dust space charge self-shielding length with $|q_d n_d/en_i|$ for $\sigma[=T_i/T_e]=0.1,0.01$. These two figures show that for $\sigma=0.1$ (Fig. 1), the transition from DA wave to DEA (DC) wave takes place at $|q_d n_d/en_i|\approx 0.35$ for hydrogen plasma ($\sqrt{m_i/m_e}\approx 42.79$), $|q_d n_d/en_i|\approx 0.45$ for oxygen plasma ($\sqrt{m_i/m_e}\approx 171.42$), $|q_d n_d/en_i|\approx 0.48$ for argon plasma ($\sqrt{m_i/m_e}\approx 271.34$), and $|q_d n_d/en_i|\approx 0.52$ for cesium plasma ($\sqrt{m_i/m_e}\approx 492.81$), whereas for $\sigma=0.01$ (Fig. 2), the transition points for the same species are 0.047, 0.052, 0.053, and 0.054, respectively. Hence for lighter plasma species the span of DEA (DC) wave is greater than that of heavier plasma species and also the span of DEA (DC) wave mode increases with the increase of ion–electron temperature ratio σ.

The system of simultaneous equations (46) has been solved numerically by the usual Runge–Kutta method with the plasma parameters $\sigma=0.01$ and $|q_d n_d/en_i|=0.5$ for which $\lambda_D^2>\lambda_c^2$ [Fig. 2, DEA (DC) wave mode]. Figure 3 shows the oscillatory nature of DEA (DC) shock wave for weak dissipation and Fig. 4 shows the monotonic nature of DEA (DC) shock wave for strong dissipation.

Measured in terms of the electron Debye length $\lambda_{\rm De}=\sqrt{\epsilon_0 T_e/n_0 e^2}$, a characteristic length independent of ion mass, let the shock width be defined by

$$L=L_\eta \Big/ \left(\frac{\lambda_{\rm De}}{\lambda_c}\right), \tag{51}$$

where

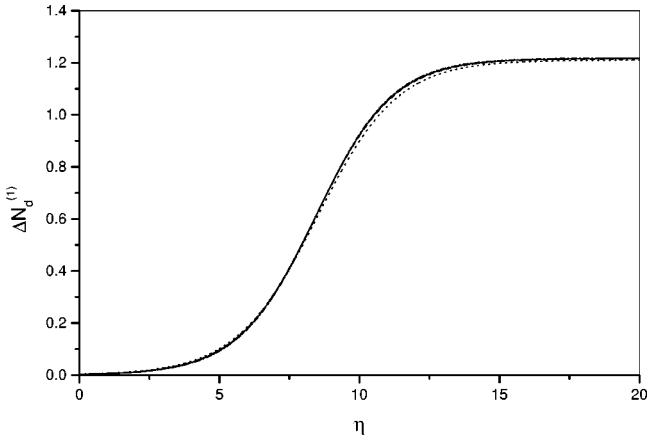

FIG. 4. Monotonic shock structure for strong dissipation for same σ and $|q_d n_d/en_i|$. $\Delta N_d^{(1)}$ is the normalized (normalized by equilibrium dust number density n_{d0}) dust number density and $\eta=\xi-V\tau$ is the transformed spatial cordinate. The curves are the same as in Fig. 1. Clearly L_η (52) is almost the same for all the curves (representing hydrogen, oxygen, argon, and cesium plasmas) but shock width L (51) varies widely being least for hydrogen and greatest for cesium plasma. The same observation applies for Fig. 3.

$$L_\eta = \eta_{f.d} - \eta_{f.u}. \tag{52}$$

Here $\eta_{f.d}(\eta_{f.u})$ is the value of η (45) corresponding to the far downstream (far upstream) value of ΔN_d. Figures 3 and 4 show that L_η is almost independent of ion mass m_i, while for any $|q_d n_d/en_i|$, λ_D/λ_c (Figs. 1 and 2) decreases and consequently the shock width L of the DEA (DC) shock wave increases monotonically. Thus for identical values of $|q_d n_d/en_i|$, the DEA (DC) shock width of hydrogen plasma is the least followed in the increasing order by those of oxygen, argon, and cesium plasma, respectively. On the other hand, the increase in ion mass has little effect on the DA shock width as λ_D^2/λ_c^2 changes only weakly with m_i for $\lambda_D^2/\lambda_c^2<1$.

Figure 5 shows the variation of shock strength given by

$$[\epsilon \Delta N_d^{(1)}]_{\max} = 2\,\frac{(M-1)}{\alpha}, \tag{53}$$

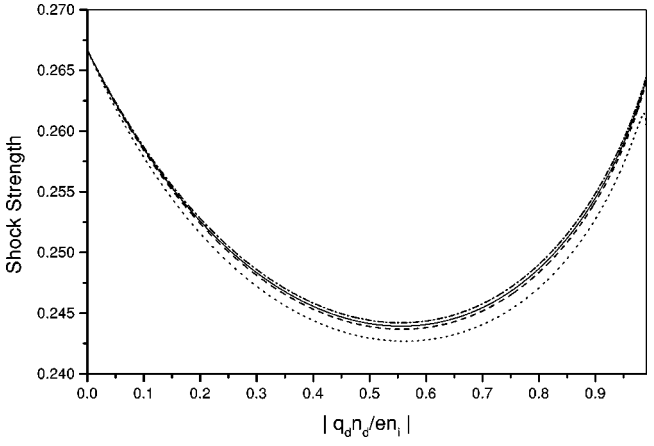

FIG. 5. Variation of shock strength [given by Eq. (53)] with $|q_d n_d/en_i|$ for $\sigma=0.1$. The curves are the same as in Fig. 1.

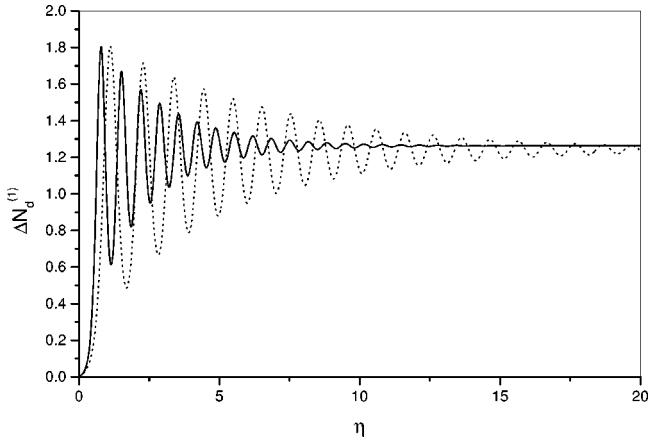

FIG. 6. Shock structures for both DA wave (solid curve, with $|q_d n_d/en_i|=0.2$ for which $\lambda_D^2/\lambda_c^2<1$) and DEA (DC) wave (dotted curve, with $|q_d n_d/en_i|=0.8$ for which $\lambda_D^2/\lambda_c^2>1$) for hydrogen plasma with $\sigma=0.1$. $\Delta N_d^{(1)}$ and η is the same as in Fig. 3.

where α is given by Eq. (43) with $|q_d n_d/en_i|$ for $\sigma=0.1$. This figure shows that the shock strength decreases initially with the increase of dust space charge density $|q_d n_d|$, near the DA wave–DEA (DC) wave transition boundary at $\lambda_D^2/\lambda_c^2=1$, assumes a minimum value and then increases continuously as the ratio of space charge density approaches unity. For DA wave the shock strength is more pronounced than that for DEA (DC) wave. This is clearly seen from Fig. 5 as shock strength has a lower value to the right of the crossover point of DA wave to DEA (DC) wave transition line $\lambda_D^2/\lambda_c^2=1$.

The shock structures for hydrogen plasma for $\sigma=0.1$ of both DA wave (solid line, $|q_d n_d/en_i|=0.2$, where $\lambda_D^2/\lambda_c^2<1$) and DEA (DC) wave (dotted line, $|q_d n_d/en_i|=0.8$, where $\lambda_D^2/\lambda_c^2>1$) have been shown in Fig. 6. This figure shows that starting from near zero value the DA shock wave reaches its steady value more rapidly than DEA (DC) shock wave. This happened due to the higher dispersion of DEA (DC) wave than that of DA wave [$\beta \propto \lambda_D^2/\lambda_c^2$ by Eq. (43)].

From all these considerations, it is seen that the transition from DA wave to DEA (DC) wave mode takes place at lower value of the ratio of dust space charge density to that of ions, i.e., $|q_d n_d/en_i|$ for $\sigma=T_i/T_e \ll 1$ and also for lighter plasma species such as hydrogen plasma. Therefore the favorable for the observation of linear as well as nonlinear DEA (DC) shock wave is rf discharge dusty plasma experiment or dusty double-plasma device with hydrogen plasma, where electrons are hotter than ions, i.e., $\sigma<1$. But for sufficiently hotter electrons than ions, i.e., for $\sigma \ll 1$, the linear and nonlinear DEA (DC) wave mode for heavier plasma species such as oxygen, argon, and cesium plasma, can also be observed in rf discharge dusty plasma experiment or dusty double-plasma device, as in the normal rf discharge dusty plasma experiment or dusty double-plasma device, the dusty plasma experiemnts are often done with $T_i \ll T_e$, i.e., $\sigma \ll 1$.

In this paper we have considered the nonadiabatic dust charge variation under the assumption that $\omega_{\rm pd}/\nu_{\rm ch} \neq 0$ where $\omega_{\rm pd}$ is the dust plasma frequency and $\nu_{\rm ch}$ is the dust

charging frequency, in a collisionless dusty plasma and this leads to the formation of DEA (DC) shock wave. However, in a collisional dusty plasma DEA (DC) shock wave may also be observed due to the dust–dust or dust–neutral collisional dissipation through dust viscosity.

[1]C. K. Goertz, Rev. Geophys. **27**, 271 (1989).
[2]A. Barkan, N. D'Angelo, and R. Merlino, Phys. Rev. Lett. **73**, 3093 (1994).
[3]B. Walch, M. Horanyi, and S. Robertson, IEEE Trans. Plasma Sci. **22**, 97 (1994).
[4]Y. Nakamura and H. Bailung, Rev. Sci. Instrum. **70**, 2345 (1999).
[5]O. Havnes, C. K. Goertz, G. E. Morfill, and W. Ip, J. Geophys. Res., [Atmos.] **92**, 2281 (1987).
[6]N. N. Rao, P. K. Shukla, and M. Y. Yu, Planet. Space Sci. **38**, 543 (1990).
[7]P. K. Shukla and V. P. Silin, Phys. Scr. **45**, 508 (1992).
[8]F. Melandso, T. Aslaksen, and O. Havnes, Planet. Space Sci. **41**, 321 (1993).
[9]A. Barkan, R. Merlino, and N. D'Angelo, Phys. Plasmas **2**, 3563 (1995).
[10]Y. Nakamura, H. Bailung, and P. K. Shukla, Phys. Rev. Lett. **83**, 1602 (1999).
[11]K. Avinash and P. K. Shukla, Phys. Plasmas **7**, 2763 (2000).
[12]K. Avinash, Phys. Plasmas **8**, 3897 (2001).
[13]N. N. Rao, Phys. Plasmas **6**, 4414 (1999).
[14]N. N. Rao, Phys. Plasmas **7**, 795 (2000); **7**, 3214 (2000).
[15]N. N. Rao and F. Verheest, Phys. Lett. A **268**, 390 (2000).
[16]F. Verheest and P. K. Shukla, Phys. Plasmas **9**, 1113 (2002).
[17]N. N. Rao and P. K. Shukla, Phys. Plasmas **8**, 370 (2001).
[18]S. Ghosh, S. Sarkar, M. Khan, M. R. Gupta, and K. Avinash, Phys. Lett. A **298**, 49 (2002).
[19]J. X. Ma and X. Liu, Phys. Plasmas **4**, 253 (1997).
[20]B. Xie, K. He, and Z. Huang, Phys. Lett. A **247**, 403 (1998).
[21]M. R. Gupta, S. Sarkar, S. Ghosh, M. Debnath, and M. Khan, Phys. Rev. E **63**, 046406 (2001).
[22]S. Ghosh, S. Sarkar, M. Khan, and M. R. Gupta, Phys. Lett. A **274**, 162 (2000).
[23]S. Ghosh, S. Sarkar, M. Khan, and M. R. Gupta, Phys. Plasmas **9**, 1150 (2002).